Dual Active Bridge Based Isolation Stage for Power Electronic Transformer

Viktor Beldjajev, Indrek Roasto
Tallinn University of Technology
vbeldjajev@gmail.com; indrek.roasto@ttu.ee

***Abstract*- This paper proposes new topology for high frequency isolation stage of power electronic transformer based on dual active bridge (DAB). The aim of the paper is to provide simplified loss analysis with efficiency evaluation. Zero voltage switching is observed with simulation results and overall efficiency is determined.**

I. INTRODUCTION

The power electronic transformer (PET), also called solid state transformer is a new type of transformer that realizes voltage transformation, galvanic isolation and power quality enhancements in a single device. The PET is suitable for the use in the power systems that comprise renewable energy sources, energy storage devices as well as different type of loads, thus the bi-directional power flow is the most important requirement that the PET has to fulfil. Different PET topologies have been analyzed in [1]-[4]. According to [3] and [5] the three stage PET topology seems to be the most promising. This topology consists of AC-DC, DC-DC and DC-AC power electronic converting stages, with a high-frequency transformer for voltage reduction or elevation. The DC-DC stage, also called an isolation stage consists of on DC-AC stage, where DC voltage is converted into high frequency AC voltage, which is transferred to the secondary side through the high frequency transformer. Afterwards the transformed AC voltage is rectified again on the transformer secondary.

A suitable and promising candidate for the isolation stage is the dual active bridge (DAB). DAB converter has a bi-directional power flow capability with a wide zero voltage switching (ZVS) range without additional circuitry. The DAB converter finds applications where high efficiency, power density and dynamic energy storage is needed, such as flywheel, battery, and ultra capacitor based energy storage for renewal energy sources, electric vehicles or smart-grid distribution. Power electronic transformer is suitable for interconnecting the renewable energy sources as well as energy storage devices and different types of loads into one system. Thus the isolation stage must provide reliable energy flow between these subsystems.

In order to facilitate a thorough the optimization of the isolation stage, the voltage and current stresses of different components (semiconductors, transformer, capacitors) and overall power dissipation need to be determined. Although semiconductor technology has improved much during last decades, the voltage blocking capability tends to be much lower than required for the HV side. To minimize the voltage and current stresses, the recent approach in PET design is using the modular structure, where the base cells are connected either in parallel or in series [5]. A series connection of one phase base cells is shown in Fig. 1.

II. DUAL ACTIVE BRIDGE

The dual active bridge converter is an isolated switching converter that allows bi-directional power flow between two DC voltage sources that may have different voltage levels, hence it can step up or down the voltage in both directions. When converter operates in forward mode, the power is transferred from high-voltage side to low voltage side. Vice versa is valid for reverse mode. As in most other converters, soft switching can also be employed to improve the efficiency of this topology. For ZVS the high leakage inductance of HF transformer is utilized.

The main circuit components of DAB are two voltage sources, two capacitors, an active full-bridge converter on the right hand side and another one on the left hand side, and high frequency transformer. DAB can be controlled using conventional modulation strategy (CMS), which was analyzed in [6]. CMS consists of controlling both bridges with a 50 % duty cycle in order to generate square wave voltage. Power flow can be controlled by controlling the phase shift between the primary and secondary side. When phase shift is positive, the power is transferred from primary side to secondary and vice versa. With adjusting the phase shift value (0…90°) the transferred power can be controlled. [6]-[7] present the constraints and requirements for achieving zero voltage switching of DAB in whole operating range. It can be concluded, that with proper modulation the switching and conduction losses can be drastically minimized. As show the research in [10] the efficiency of higher than 90% can be achieved.

DAB operates at a high frequency, which improves the power density and the circuit performance, however rising the frequency causes higher switching losses. High switching frequencies in PWM converters are limited by: (i) switching stress (high voltage and current peaks) during the turn-on, turn off transients; (ii) switching losses; (iii) severe *di/dt* and *du/dt* produce electromagnetic interference [11]. The main goal is to achieve the 40 kHz switching frequency of the IGBT-s.

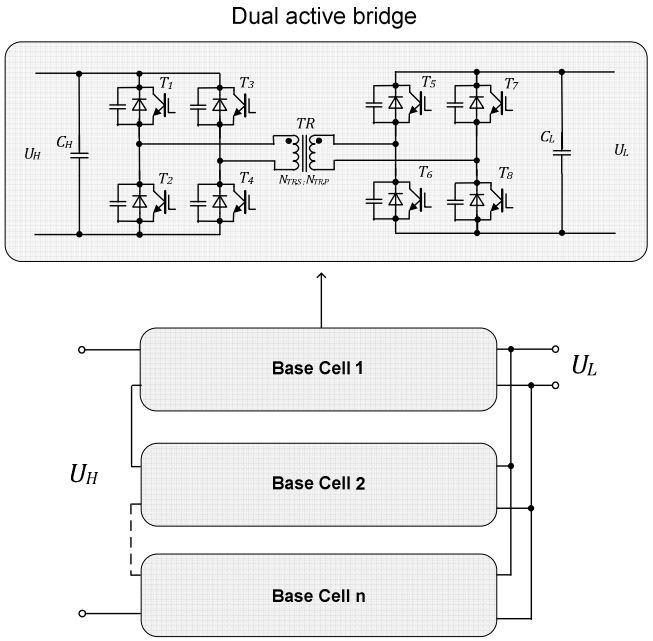

Fig. 1. Modular structure of power electronic transformer with DAB based isolation stage.

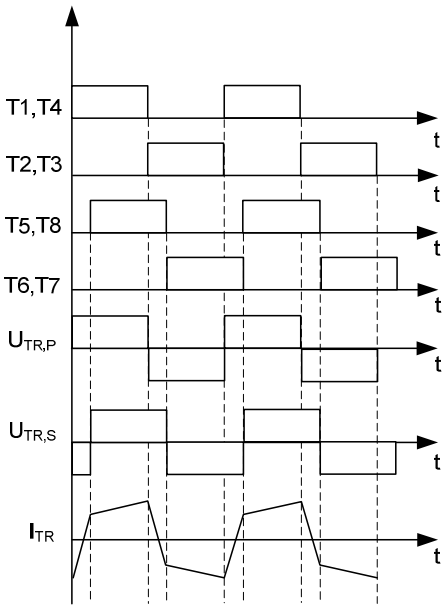

Fig. 2. Gate signals, transformer primary and secondary voltages, as well as transformer current waveforms.

III. PRINCIPLE OF OPERATION

In DAB the primary and secondary side bridges are controlled simultaneously. Primary bridge consists of transistors T1…T4. The gate signals are same for T1 and T4, whereas the gate signals for T2 and T3 are complementary signals with 50 % duty cycle. The secondary bridge is controlled in a similar way, however the gate signals are phase shifted by value of phase angle φ respectively. Each bridge generates two phase shifted voltages (V_1 and V_2), which in turn generate a voltage V_μ over the leakage inductance of the HF transformer. This voltage causes current to flow from one bridge to another extracting this way energy simultaneously from both converter sides.

During positive half-cycle the current rate change is determined by

$$\frac{di}{dt} = \frac{V_1 + V_2}{L} \tag{1}$$

when the rapid increase in transformer current can be observed. Current increases until the phase shift angle φ is reached. Afterwards the current will increase with a smoother slope accordingly to the rate

$$\frac{di}{dt} = \frac{V_1 - V_2}{L}. \tag{2}$$

During negative half-cycle the current rate increase is determined in a similar way. First according to

$$\frac{di}{dt} = \frac{-V_1 - V_2}{L} \tag{3}$$

and after phase shift angle φ is achieved the current rate is determined as follows

$$\frac{di}{dt} = \frac{-V_1 + V_2}{L}. \tag{4}$$

The waveforms of gate signals, primary and secondary phase shifted voltages as well as the transformer current is shown in Fig. 2.

IV. LOSS ANALYSIS

For the following simple loss analysis it is assumed that converter is operating at its optimal point. The influences of skin and proximity effects on the conduction losses of power electronic switches and transformer, as well as PCB capacitance and gate driver losses are neglected.

A. Core Losses

Core losses occur in the high-frequency transformer and can be obtained accordingly to Steinmetz equation [12].

$$P_{core} \approx V_{core} k f_S^{\alpha} B_{tr,peak}^{\beta} \tag{5}$$

where k, α, β are the Steinmetz parameters. Researchers have shown that core losses are less than 10 % of the total losses (at rated output power).

B. Conduction Losses

The conduction losses in the switches are determined by the RMS currents. The switches in both converters consist of an IGBT, an anti-parallel diode and a capacitor. In steady-state operation, every switch conducts current with duty cycle of 50%, whereas the transformer current $i_L(t)$ repeats with negative sign after one half-cycle. Since every switch conducts current during the half cycle, the RMS current is easily obtained from transformer current $i_L(t)$

$$I_{rms} = \frac{I_L}{\sqrt{2}}, \tag{6}$$

and the secondary side switches carry the current

$$I_{TS,DAB} = \frac{n \cdot I_L}{\sqrt{2}} . \quad (7)$$

For an IGBT the conduction losses can be evaluated as follows

$$P_{con} = I_{RMS}^2 \cdot R_{CE} , \quad (8)$$

where R_{CE} is the resistance of an IGBT. The conduction losses of the diodes are evaluated in a similar way

$$P_{D,CON} = I_{avg} \cdot U_f , \quad (9)$$

where I_{avg} is the average current in the diode and U_f is forward voltage drop over the diode.

Conduction losses for the HF transformer can be obtained as follows

$$P_{tr,con} = (R_p + n^2 R_s) I_L^2 \quad (10)$$

where R_p and R_S are primary side and secondary side winding resistances respectively. Table 1 sums up the conduction losses of the whole converter.

TABLE I

TOTAL CONDUCTION LOSSES OF DAB

	Primary Side	**Secondary Side**
Losses	$4 \cdot P_{con,p} + P_{tr,con}$	$4 \cdot P_{con,s}$

C. Switching Losses

Switching losses occur when electronic switches turn on and off, and they can constitute a large part from the total losses. The switching losses P_{SW} can be minimized when zero voltage switching (ZVS) or zero current switching (ZCS) is achieved. On the contrary, the hard switching losses lead to excessive semiconductor losses and must be avoided. There are two basic constraints for the soft switching to be realized:

a) at turn on of any device its anti-parallel connected diode is conducting,

b) at turn off of any device the minimum current through the device is zero.

According to [13] the switching losses of the power switches can be evaluated as follows

$$P_{SW} = \frac{1}{2} V_S I f_S (t_{on} + t_{off}) \quad (11)$$

where V_S is the supply voltage, I is the steady-state current, f_s is switching frequency, t_{on} and t_{off} turn-on and turn-off times respectively. Thus, the switching losses vary linearly with the switching frequency and the switching times. Therefore, if high switching frequencies are required, the devices should have short switching times to keep the switching losses as low as possible. If ZVS at turn-on is achieved then only the turn-off losses are needed to be taken into account.

For IGBT-s the turn-off loss cannot be totally avoided due to the stored charge caused by minority carrier injection, which cannot be removed by the gate driver. These excessive carriers must be forced out by additional transistor current.

D. Total Losses

Total losses of the DAB converter comprise the core losses, the conduction losses on the transformer windings as well as in the active resistance of the switches. Also the switching (turn-off) losses of the switches are present. For DAB the total losses in forward and reverse operating modes are evaluated as follows

$$P_{DAB} = 4P_{con,p} + P_{tr,con} + P_{core} + 4P_{con,s} + 8P_{SW} . \quad (12)$$

V. SIMULATION RESULTS

The aim of the simulation was to determine the overall efficiency of the converter and ensure that the ZVS is achieved in every leg of DAB. The DAB circuit was simulated in PSIM environment with parameters presented in Table 2. During the simulation, the converter was operating in the forward mode (positive phase shift angle). As can be seen in Fig. 3, ZVS is achieved in both, leading and lagging legs on primary and secondary sides of the converter, since diodes of corresponding switches are conducting at the moment when transistor turns on. All switches are turned-off under hard switching conditions.

For the overall efficiency evaluation the input and the output power were measured at the steady-state operating point. The input power comprised P_{in} = 2940 W and the output power was P_{out} = 2730 W. Using the general efficiency evaluation formula

$$\eta = \frac{P_{OUT}}{P_{IN}} \quad (13)$$

the calculated efficiency of the converter was estimated to be 93 % which is an expected efficiency for the isolation stage of PET, however several strategies exist that could improve the efficiency even more. For example, a research in [7] proposes new modulation strategy that allows extending the soft switching region over whole operating range and reducing the reactive power consumption, thus reducing this way the switching as well as conduction losses. Also triangular and trapezoidal modulation of DAB can be used for the control.

TABLE 1

SIMULATION CIRCUIT PARAMETERS FOR DAB

Parameter	**Value**
Low side voltage (U_L)	350 V
High side voltage range (U_H)	700 V
Power (P)	3 kW
Switching frequency (f_s)	12 kHz
HF transformer turns ratio (N_{TR})	2
Leakage inductance of HF transformer (L_μ)	10 μH
Transformer winding resistance (R_{TR})	1 mΩ
IGBT voltage drop (U_{IGBT})	1,2 V
Diode voltage drop (U_D)	0,3 V
Phase shift (φ)	30 deg
Duty cycle (D)	0.5

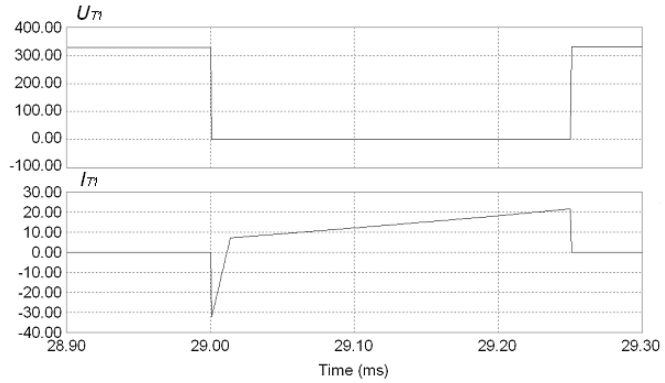

a)

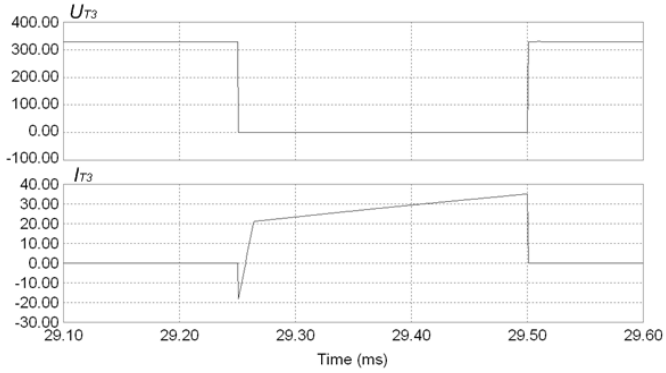

b)

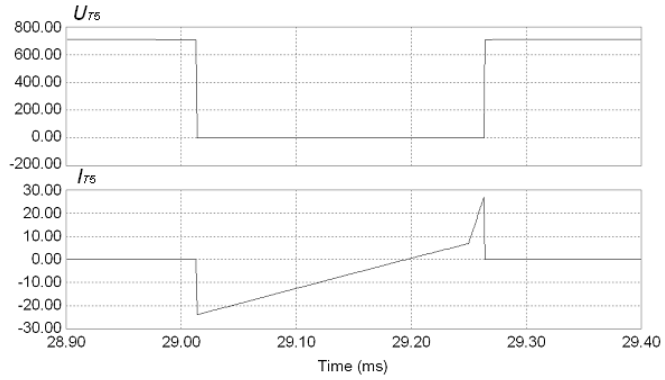

c)

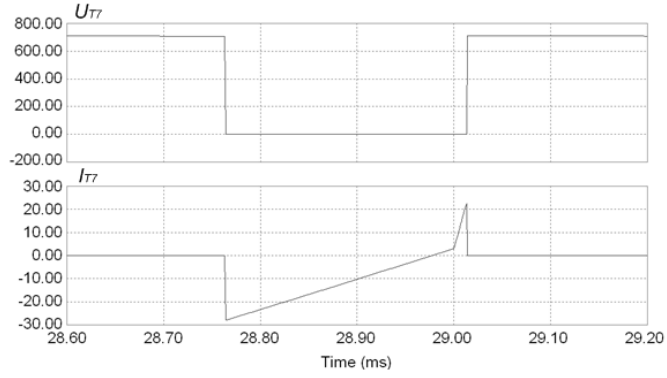

d)

Fig. 3. ZVS sequence of the DAB all four legs: a – primary leading leg; b – primary lagging leg; c – secondary leading leg, d – secondary lagging leg.

CONCLUSION

This paper proposed a dual active bridge based dc/dc converter for new power electronic transformer. According to simulation results, the zero voltage switching at turn-on occurs in all four legs of the converter. ZVS has a strong impact on the overall efficiency of the converter. The achieved efficiency of 93%, however research has stated that with proper modulation the switching and conduction losses can be minimized even more. Future work will comprise the accurate loss analysis and current and voltage stress determination and their experimental verification.

ACKNOWLEDGEMENT

This research and work has been supported by Estonian Ministry of Education and Research (Project SF0140016s11), Estonian Science Foundation (Grant ETF8687) and Estonian Archimedes Foundation (Project “Doctoral School of Energy and Geotechnology II”).

REFERENCES

[1] van der Merwe, J.W.; du T. Mouton, H.; , "The solid-state transformer concept: A new era in power distribution," *AFRICON, 2009. AFRICON '09.* , vol., no., pp.1-6, 23-25 Sept. 2009.

[2] Heinemann, L.; Mauthe, G.; , "The universal power electronics based distribution transformer, an unified approach," *Power Electronics Specialists Conference, 2001. PESC. 2001 IEEE 32nd Annual* , vol.2, no., pp.504-509 vol.2, 2001.

[3] Falcones, S.; Xiaolin Mao; Ayyanar, R.; , "Topology comparison for Solid State Transformer implementation," *Power and Energy Society General Meeting, 2010 IEEE* , vol., no., pp.1-8, 25-29 July 2010.

[4] Hengsi Qin; Kimball, J.W.; , "A comparative efficiency study of silicon-based solid state transformers," *Energy Conversion Congress and Exposition (ECCE), 2010 IEEE* , vol., no., pp.1458-1463, 12-16 Sept. 2010.

[5] Beldjajev, V.; Roasto, I.; Lehtla T.; , “Intelligent Transformer: Possibilities and Challenges” RTU, 2011. , pp . 14 Okt 2011.

[6] De Doncker, R.W.A.A.; Divan, D.M.; Kheraluwala, M.H.; , "A three-phase soft-switched high-power-density DC/DC converter for high-power applications," *Industry Applications, IEEE Transactions on* , vol.27, no.1, pp.63-73, Jan/Feb 1991

[7] Oggier, G.G.; García, G.O.; Oliva, A.R.; , "Modulation Strategy to Operate the Dual Active Bridge DC–DC Converter Under Soft Switching in the Whole Operating Range," *Power Electronics, IEEE Transactions on* , vol.26, no.4, pp.1228-1236, April 2011

[8] Kheraluwala, M.H.; Gasgoigne, R.W.; Divan, D.M.; Bauman, E.; , "Performance characterization of a high power dual active bridge DC/DC converter," *Industry Applications Society Annual Meeting, 1990., Conference Record of the 1990 IEEE* , vol., no., pp.1267-1273 vol.2, 7-12 Oct 1990

[9] Alonso, A.R.; Sebastian, J.; Lamar, D.G.; Hernando, M.M.; Vazquez, A.; , "An overall study of a Dual Active Bridge for bidirectional DC/DC conversion," *Energy Conversion Congress and Exposition (ECCE), 2010 IEEE* , vol., no., pp.1129-1135, 12-16 Sept. 2010

[10] Krismer, F.; Kolar, J.W.; , "Accurate Power Loss Model Derivation of a High-Current Dual Active Bridge Converter for an Automotive Application," *Industrial Electronics, IEEE Transactions on* , vol.57, no.3, pp.881-891, March 2010

[11] Bellar, M.D.; Wu, T.S.; Tchamdjou, A.; Mahdavi, J.; Ehsani, M.; , "A review of soft-switched DC-AC converters," *Industry Applications, IEEE Transactions on* , vol.34, no.4, pp.847-860, Jul/Aug 1998

[12] Reinert, J.; Brockmeyer, A.; De Doncker, R.W.; , "Calculation of losses in ferro- and ferrimagnetic materials based on the modified Steinmetz equation," *Industry Applications Conference, 1999. Thirty-Fourth IAS Annual Meeting. Conference Record of the 1999 IEEE* , vol.3, no., pp.2087-2092 vol.3, 1999

[13] Oliva, A.; Ang, S.; , “Power-Switching Converters,” Third Edition, CRC Press New York, US, 2011.